Kumar et al. 2018. *Int. J. Vehicle Structures & Systems*, 10(1), 30-34
ISSN: 0975-3060 (Print), 0975-3540 (Online)
doi: 10.4273/ijvss.10.1.07

International Journal of Vehicle Structures & Systems
Available online at www.maftree.org/eja

Experimental Evaluation of Magnetorheological Damper Characteristics for Vibration Analysis

S. Siva Kumar[a], K.S. Raj Kumar and Navaneet Kumar

Dept. of Aeronautical Engg., Bharath Institute of Higher Education and Research, Chennai, India
[a]Corresponding Author Email: svkmr_s@yahoo.co.in

ABSTRACT:

Magnetorheological (MR) fluid damper has been designed, fabricated and tested to find the stiffness and damping characteristics. Experimentally the MR damper has been tested to analyse the behaviour of MR fluid as well as to obtain the stiffness for varying magnetic field. MR damper mathematical model has been developed for evaluating dynamic response for experimentally obtained parameters. The experimental results show that the increase of applied electric current in the MR damper, the damping force will increase remarkably up to the saturation value of current. The numerical simulation results that stiffness of the MR damper can be varied with the current value and increase the damping forces with the reduced amplitude of excitation. Experimental and theoretical results of the MR damper characteristics demonstrate that the developed MR damper can be used for vibration isolation and suppression.

KEYWORDS:

Magnetorheological fluid damper; Stiffness; Damping force; Semi active; Vibration

CITATION:

S.S. Kumar, K.S.R. Kumar and N. Kumar. 2018. Experimental Evaluation of Magnetorheological Damper Characteristics for Vibration Analysis, *Int. J. Vehicle Structures & Systems*, 10(1), 30-34. doi:10.4273/ijvss.10.1.07.

1. Introduction

Magnetorheological (MR) fluid controllable structures and system components are well established for commercial applications. The development of MR fluid system components used in suspensions for automobiles, trains, helicopter rotor assembly, pilot seats, cable stayed bridges, high buildings etc. for attenuating vibrations. MR fluid isolator was developed by Zhou et al [1] and investigated the dynamic behaviour under various magnetic fields. The MR isolator stiffness and damping coefficient and their performance characteristics were evaluated by numerical simulation. Shixinga et al [2] fitted the MR damper in the landing gear and carried out a drop test to analyze the performance and the application in practice. Yao et al [3] presented Bouc-Wen model to characterize the performance of the MR damper, with optimization method in Matlab. Aslam et al [4] studied the properties of MR fluids and their applications in suspensions of vehicles, trains, tall buildings, cable-stayed bridges and dampers. Zareh et al [5] investigated a novel intelligent semi-active control system for eleven degrees of freedom passenger car's suspension system using MR damper with neuro-fuzzy control strategy to enhance the desired suspension performance.

Kim et al [6] tested a large bus suspension to measure its dynamic response by the single-lane change test and the rapid stop test. A full car model is established by ADAMS/Car for computer simulation. Prabakar et al [7] presented a control strategy for the stationary response of a quarter car model to random road excitation using a MR damper as a semi active suspension and analyzed using multi-objective optimization technique. Powell et al [8] investigated fluid composites and their performance for potential use in helicopter landing gear applications. Liao et al [9] developed a single degree of freedom system suspension with the MR damper to provide effective damping for vibration control. Murakami et al [10] developed an evaluation method for the damping force characteristics of a passive-type MR damper with functional equivalent to semi active system. Current research is attempting to find the stiffness and damping characteristics of low cost and efficient MR damper and to be used in the suspensions for automobiles and aircrafts.

2. Design, fabrication and assembly

The MR damper consists of main cylinder, piston, magnetic circuit and MR fluid. The designing of the damper has been done with the parameters as given in Table 1. The piston rod and head draft diagram with the dimensions are shown in Figs. 1 and 2. The design of damper was performed using CATIA V5. Solid model of piston rod and head is shown in Fig. 3. Silicon oil is used as the carrier fluid in the MR damper. Silicon oil works more efficient when the iron particles are mixed up properly with the carrier fluid. The magnetic particles size ranging from 3 to 5 microns has been used to achieve yield strengths upto 50-100 kPa at magnetic field strength of about 150-250 kA/m. The composition of the fluid is taken in such a way that of every 200-250ml, only 40 g of iron particles can be mixed up. The fabricated components and their assembly of the MR damper are shown in Fig. 4.

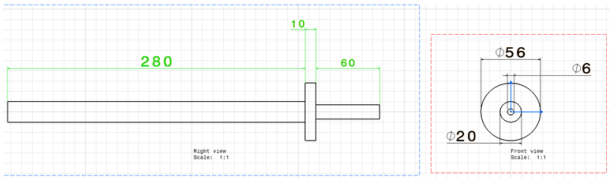

Fig. 1: Piston rod diagram (dimensions are in mm)

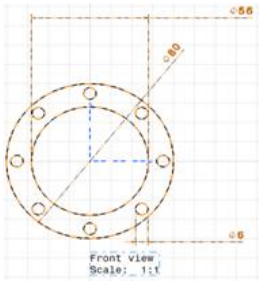

Fig. 2: Piston head diagram (dimensions are in mm)

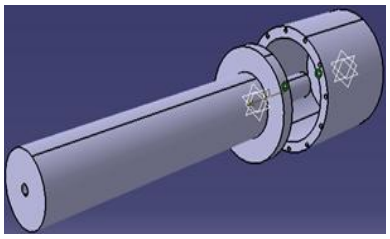

Fig. 3:.Solid modelling of piston rod and head

Table 1: MR damper parameters

Parameter	Value
Pole length(L), cm	4.6
Poles distance(l), cm	1.1
Piston radius (R), cm	4.8
Piton rod radius(r), cm	3.7
Total damper length (Lt), cm	28.0
Clearance between piston & cylinder(t), cm	0.02
Cylinder thickness (t), cm	0.04
MR damper mass, kg	8.0

Fig. 4: Manufactured components and assembly of MR damper

3. Test setup and results

Fig. 5 shows the experimental set up by using universal testing machine with different voltage to achieve the characteristics of MR fluid. The damper (see Fig. 6) was tested with different voltages through 12V battery. The voltage supplied to the damper has been controlled by rheostat. A multimeter is connected to check the given supply to the armature inside the piston assembly of the damper. At first the coil wound in the piston assembly is supplied with the current of 2A for the magnetization of the MR fluid that flow through the piston. The current level was then changed incrementally to 2.5A to 4A. Then the load was applied on the damper. The MR fluid characteristics at electric current of 1A, 2.5A, 3.5A and 4A are shown in Fig. 7 to Fig. 10 respectively. The fluid viscosity changes due to increased current and magnetic field in the piston region. When the applied current is more than 4.2A the increase of damping force is no longer significant this means that saturation occurs at 4.2A. The max. load carrying capacity has increased from 5.2 kN to 11.5 kN of the damper for an applied current from 2.5A to 4A.

Fig. 5: Experimental setup

Fig. 6: MR damper prototype

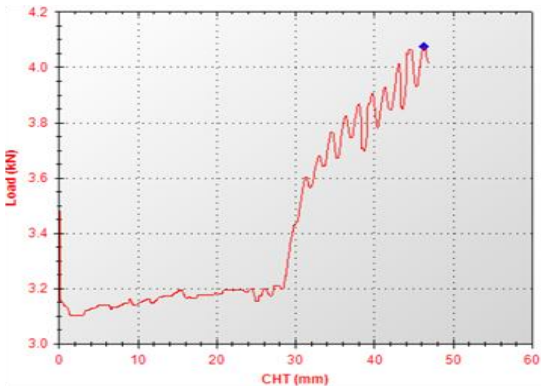

Fig. 7: Effect of damping force at 2 A

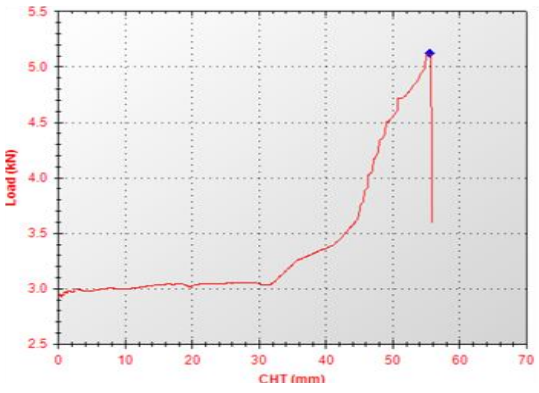

Fig. 8: Effect of damping force at 2.5 A

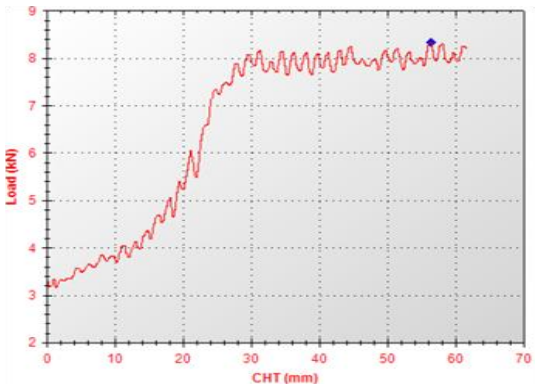

Fig. 9: Effect of damping force at 3.5 A

Fig. 10: Effect of damping force at 4 A

4. Mathematical model

The fabricated MR damper has been mathematically modelled as two degrees of freedom model to capture its dynamic response. Fig. 11 shows the mathematical model of a MR damper for semi active control. The outer cylinder of damper is taken as model consists of two solid masses m_1 and m_2 denoting the sprung and un-sprung masses respectively. The aircraft body mass and upper parts of the landing gear are represented by the sprung mass m_1. The mass of the wheel components are represented by the un-sprung mass m_2. These values are 8800kg and 260kg respectively. The landing gear strut which supports the body mass are represented by a linear spring with stiffness k_1 and the MR damper with a variable viscous damping coefficient c_1. The unsprung mass comes in contact with the road profile through the tire, which is represented by a spring of stiffness k_2. A damper with damping coefficient of c_2 can be added to the model in parallel to k_2 to represent the damping in the tire.y_1 and y_2 are the vertical motion of the sprung mass and unsprung mass. y_g is the ground excitation.

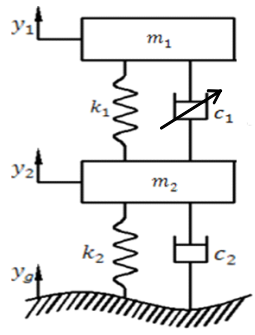

Fig. 11: Mathematical model of semi active landing gear

The model has been assumed to have a small motion in the vertical direction. Hence, the behaviour of springs, dampers and tire are assumed as linear. In this model, tire damping is also considered and the ground contact is maintained. The dynamic equations are written by using the free body diagram concept of sprung mass m_1 and unsprung mass m_2 by the Newton method. The second order differential equations for the dynamics of passive landing gear can be described as follows:

$$m_1 \ddot{y}_1 + c_1 (\dot{y}_1 - \dot{y}_2) + k_1(y_1 - y_2) = 0 \quad (1)$$

$$m_2 \ddot{y}_2 + c_1 (\dot{y}_2 - \dot{y}_1) + c_2(\dot{y}_2 - \dot{y}_g) + k_1(y_2 - y_1) + k_2(y_2 - y_g) = 0 \quad (2)$$

$$\begin{bmatrix} m_1 & 0 \\ 0 & m_2 \end{bmatrix} \begin{Bmatrix} \ddot{y}_1 \\ \ddot{y}_2 \end{Bmatrix} \begin{bmatrix} c_1 & -c_1 \\ -c_1 & c_{1+}c_2 \end{bmatrix} \begin{Bmatrix} \dot{y}_1 \\ \dot{y}_2 \end{Bmatrix} + \begin{bmatrix} k_1 & -k_1 \\ -k_1 & k_{1+}k_2 \end{bmatrix} \begin{Bmatrix} y_1 \\ y_2 \end{Bmatrix} + \begin{bmatrix} 0 \\ c_2 y_{g-} k_2 y_g \end{bmatrix} = 0 \quad (3)$$

The landing gear model parameters are taken from Fokker aircraft [5] in which the experimentally obtained parameters of MR damper as given in Table 2 are used for the numerical simulation to analyze the vibration parameters of the semi active landing gear.

These parameters will yield the frequency for the body mode and the wheel mode as follows,

$$f_s \cong \frac{1}{2\pi}\sqrt{\frac{k_1}{m_1}} \quad (4)$$

$$f_{us} = \frac{1}{2\pi}\sqrt{\frac{k_2+k_1}{m_2}} \quad (5)$$

Assuming the sprung mass damping ratio ε_1=0.35. The landing gear damping coefficient is given by,

$$c_1 = \varepsilon_1 2\sqrt{k_1 m_1} \quad (6)$$

The unsprung mass damping ratio and the tire damping coefficient are given by,

$$\varepsilon_2 = \frac{c_1}{2\sqrt{(k_1+k_2)m_2}} \quad (7)$$

$$c_2 = \varepsilon_2 2\sqrt{k_2 m_2} \quad (8)$$

The unsprung mass tire stiffness rate and damper rate as obtained from experiment are 1590 kN/m and 3.7411 Ns/m respectively.

Table 2: Semi active system obtained model parameters

Sprung mass stiffness rate, kN/m	Sprung damper rate, kNs/m	Current value, A	Body mode freq., Hz	Wheel mode freq., Hz
280	41.952	2.5	0.7738	13.24
402	59.329	3.5	1.084	13.93
600	72.663	4.0	1.314	14.61

5. Damper stiffness effect

The analysis was done by varying the damper stiffness while maintaining all other parameters were constant. The damper stiffness changes while applying the current from 2.5A to 4A. The maximum value of current applied to the component is 4.4A beyond which the armature coil is damaged. The semi active landing gear response is tested with an assumed half sine type runway bump of height 0.06m and wave length 44m (0.8*55m/s) over which the airplane travels. The excitation frequency based on the vehicle speed and the wavelength is computed as approximately 1.25 Hz (7.85rad/sec). The

sprung mass response to a bump input shows that as the stiffness increases, there is an increase in the amplitude of acceleration, velocity and displacement as shown in Figs. 12 to 14.

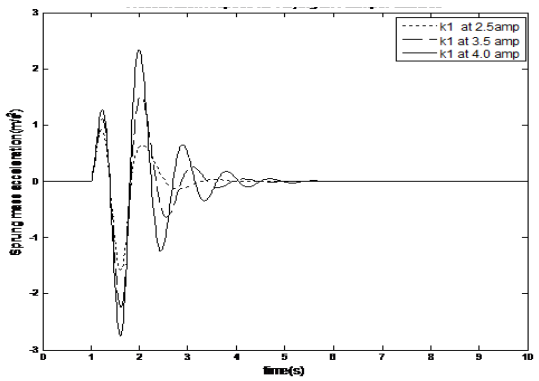

Fig. 12: Acceleration response for varying stiffness

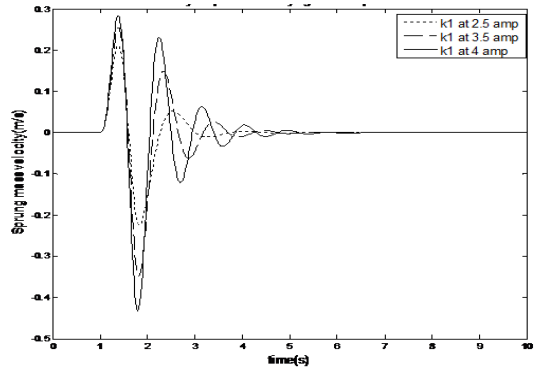

Fig. 13: Velocity response for varying stiffness

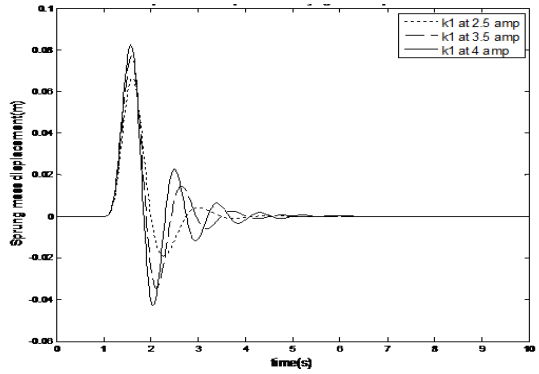

Fig. 14: Displacement response for varying stiffness

6. Damping coefficient effect

The model damping coefficient was changed due to the applied current to the damper while all other aircraft parameters are maintained as constant. The sprung mass response to a bump input shows that the semi active landing gear damping increases, the body mode is more damped, with no change to the natural frequency with reduced amplitude. The settling time is very less due to an increase in damping characteristic of the damper. The acceleration, velocity and displacement values are reduced while increasing the current and thereby increase the damping quality of the semi active system as shown in Figs. 15-17.

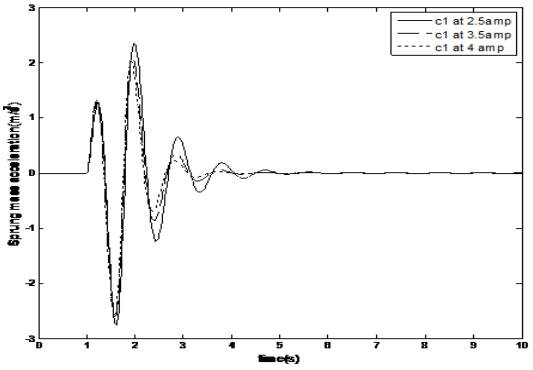

Fig. 15: Acceleration response for varying damping coefficient

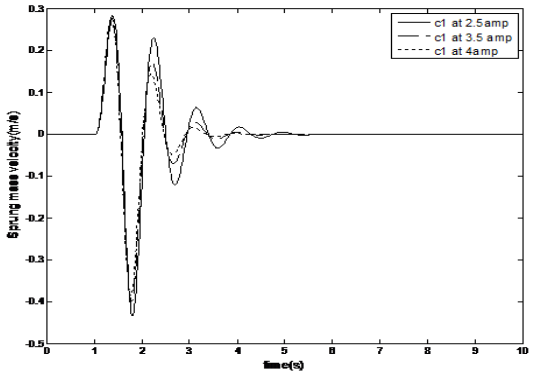

Fig. 16: Velocity response for varying damping coefficient

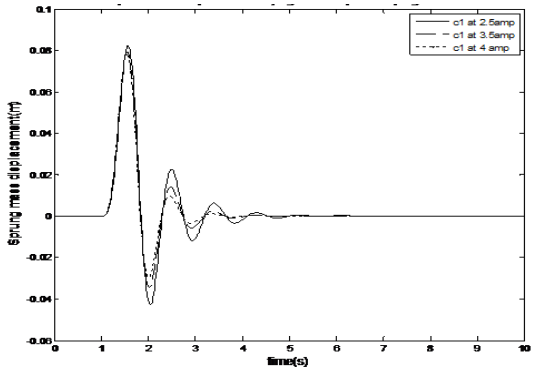

Fig. 17: Displacement response for varying damping coefficient

7. Conclusion

From the experimental and numerical simulation, the results have shown that there is a change in damping force due to variation in magnetic field. The damping coefficient increases with the increasing electric current, but decreases in excitation amplitude due to the damping force. The experiment result shows that stiffness of the MR damper can be adjusted relatively by adjusting the current. It has been found that the developed MR damper is saturated when the current reaches a threshold value of about 4.2A. Further work will look into the possible application of the developed MR damper for vibration damping of semi active landing gear system.

REFERENCES

[1] Y. Zhou, X. Wang, X.Z. Zhang and L. Weihua. 2009. Variable stiffness and damping magnetorheological isolator, *Frontiers of Mech. Engg.*, 4(3), 310-315. https://doi.org/10.1007/s11465-009-0039-4.

Z. Shixinga, W. Penga and T. Jinga. 2011. Experimental research on aircraft landing gear drop test based on MRF damper, *Procedia Engg.*, 15, 4712-4717. https://doi.org/10.1016/j.proeng.20 11.08.882.

[3] G.Z. Yao, F.F. Yap, G. Chen, W.H. Li and S.H. Yeo. 2002. MR damper and its application for semi-active control of vehicle suspension system, *Mechatronics*, 12(7), 963-973. https://doi.org/10.1016/s0957-4158(01) 00032-0.

[4] M. Aslam, Y.X. Liang and D.Z. Chao. 2006. Review of magneto rheological (MR) fluids and its applications in vibration control, *J. Marine Science & Application*, 5(3), 17-29. https://doi.org/10.1007/s11804-006-0010-2.

[5] S.H. Zareh, A. Sarrafan, A.A.A. Khayyat and A. Zabihollah. 2012. Intelligent semi-active vibration control of eleven degrees of freedom suspension, *J. Mech. Science & Tech.*, 26(2), 323-334.

[6] Y.K. Kim, S. Choi, J. Lee, W. Yoo and J. Sohn. 2011. Damper modeling for dynamic simulation of a large bus, *Int. J. Automotive Tech.*, 12(4), 521-527. https://doi.org/10.1007/s12239-011-0061-5.

[7] R.S. Prabakar, S. Sujatha and S. Narayanan. 2013. Response of a quarter car model with optimal magneto rheological damper parameters, *J. Sound & Vibration*, 332, 2191-2206. https://doi.org/10.1016/j.jsv.2012.08. 021.

[8] L.A. Powell, W. Hu and N.M. Wereley. 2013. Magneto rheological fluid composites synthesized for helicopter landing gear applications, *J. Intelligent Material Systems & Structures*, 24(9), 1043-1048. https://doi.org/10.1177/ 1045389X13476153.

[9] W.H. Liao and C.Y Lai. 2002. Harmonic analysis of a Magnetorheological damper for vibration control, *J. Smart Materials & Structures*, 11(2), 288-296. https://doi.org/10.1088/0964-1726/11/2/312.

[10] T. Murakami and M. Nakano. 2011. Numerical evaluation method for semi active damping characteristics of a passive-type MR damper with functional damping force, *J. Intelligent Material Systems & Structures*, 22(4), 327-336. https://doi.org/10.1177/ 1045389X11399941.